Coherent Structures, Particular Points and Mixing.

Florimond Guéniat
florimond@gueniat.fr

December 2014

Department of Mechanical Engineering, Florida State University

Hydrodynamic systems

Both open and confined flows are complex, and has potentially an infinite number of DoF, but coherent structures seem to play a major role.

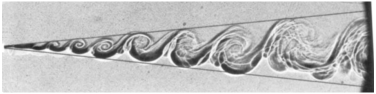

Brown & Roshko, (1974), *J. Fluid Mech.*

What is a coherent structure (see *e.g.* Chassaing, Hussain, Lumley ...) ?

- spatially localized
- significant contribution to the kinetic energy
- significant life-time
- recurrent phenomenon
- material frontiers
- etc.

Von 'Heartman' street
Isla Socorro ($Re > 10^{10}$!).

"In principle, concepts like coherent structures are best left implicit."

Hussain, (1986) *Phys. Fluids.*

Several relevant frameworks exist to identify coherent structures.

Modal framework

The aim is to give a relevant representation of a dataset, *e.g.* the energy (POD) or the frequencies (Fourier).

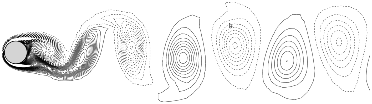

Cylinder wake

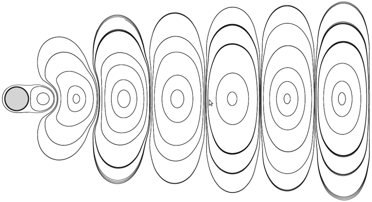

POD mode 1

Bergmann & Cordier, (2008) *J. Comput. Phys.*

Modal framework

The aim is to give a relevant representation of a dataset, *e.g.* the energy (POD) or the frequencies (Fourier).

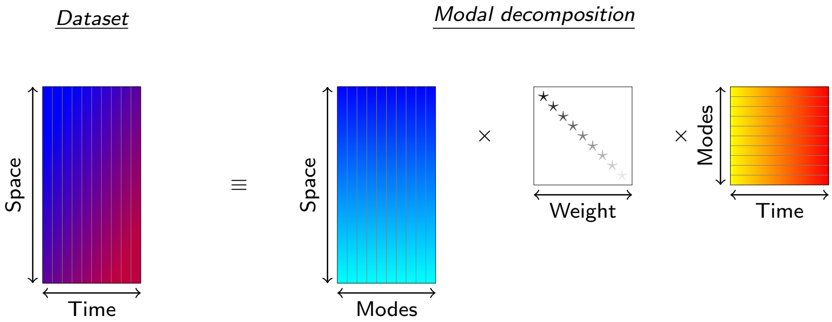

It may lead to model reduction, through Galerkin-projection or truncature.

Lagrangian framework

In fluid mechanics :

$$\dot{\boldsymbol{X}} = \boldsymbol{u}(\boldsymbol{X}, t)$$

with $\boldsymbol{X} \in \mathcal{R}^3$

$\boldsymbol{u}$ comes from DNS or PIV measurement.

$\nabla \cdot \boldsymbol{u} = 0$ implies the system is conservative (within dynamical system frame).

If the system is autonomous or periodic, then the dynamic is driven by invariant manifolds.

Lagrangian framework

In autonomous system, stable and unstable manifolds :

- are attached to a fixed point
- are invariant
- are material frontiers
- are edges of invariant sets
- drive transport and mixing
- are hyper planes of locally maximum stretching

Big data

Understand fluid mechanics

- Numerous fields/points of view
  - Velocity
  - Pressure
  - Temperature
  - Concentration ...
- Large 3DnC simulations
- Hi-Res experimental snapshots

Leads to huge dataset

- number of points : $c \times n^d \times N$

with typically

	c	d	N	n
DNS	5	3	1000	124
Exp	2	2	10000	1000

How to efficiently identify coherent structures/most relevant components from such a dataset ?

Aims of this presentation

- An (brief) introduction to dynamic modes decomposition
- Ways for identifying dynamical relevant points
  - most representative points
  - most observable points
- An introduction to lagrangian coherent structures
- Building ROM for characterizing areas of mixing in turbulent flows.

Outline

- Introduction
- Presentation of the cavity flow
- Spectral decomposition of a dataset
  - Dynamic Mode Decomposition
  - Non-Uniform DMD
- DMD-Observability
- Lagrangian Coherent Structures
- Conclusion and openings

– Cavity flow –

"Despite the diversity of types of cavity oscillations, several common features can be observed. This suggests that a general framework for describing cavity-type oscillations may be established."

Donald Rockwell, (1978) *J. Fluids Eng.*

A complex flow, still to be understood, and suited for applying methods.

Cavity flow

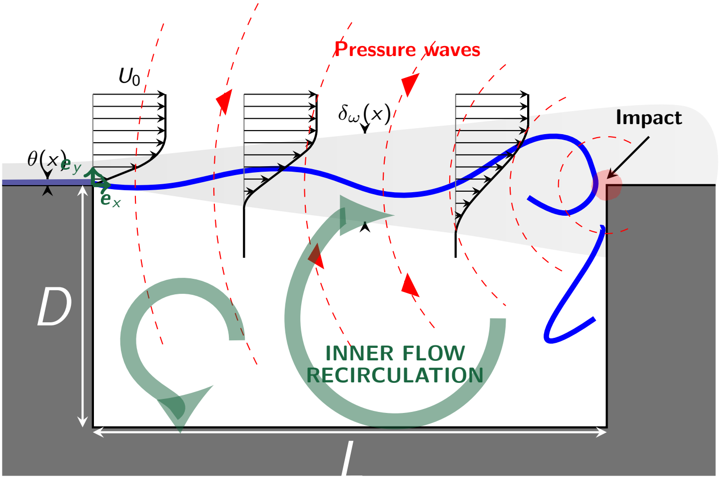

Pressure waves
U_0
$\delta_\omega(x)$
Impact
$\theta(x)$
e_y
e_x
D
INNER FLOW
RECIRCULATION
L

Cavity flow

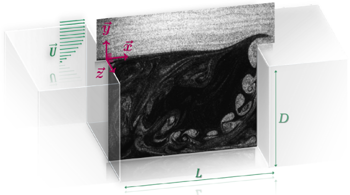

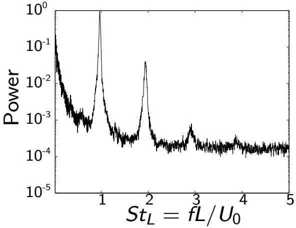

This frequency corresponds to the selected shear layer instability.

– Dynamic Modes Decomposition (DMD) –

What are dynamic modes ?

Schmid [1] ; Rowley [2] ;
→ Assume there exists an operator of evolution, A, such as the $\boldsymbol{u}_k$ are realisations of a *nonlinear* process.

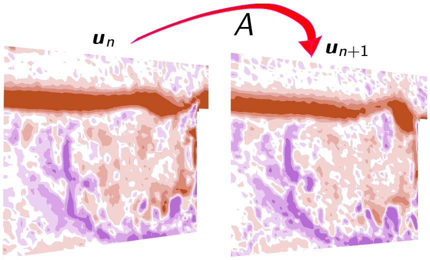

→ Find a similar matrix to A. *Dynamic modes are defined as eigenvectors of A*, computed thanks to the similar matrix.

1. Schmid *et al* (2008) *66th APS meeting* ; Schmid, (2010) *J. Fluid Mech.*
2. Rowley *et al*, (2009) *J. Fluid Mech.*

Defining the Evolution Operator A [PoF2014a]

If ϕ is the flow of the fluid dynamical system :

$$\boldsymbol{X}_{n+1} = \phi_{\Delta t} \boldsymbol{X}_n,$$

and Π is the projector onto the experimental space (*i.e.* $\boldsymbol{u}_n = \Pi \boldsymbol{X}_n$), A is defined by :

$$A \circ \Pi = \Pi \circ \phi_{\Delta t}.$$

Then,

$$\begin{aligned} A\boldsymbol{u}_n &= A \circ \Pi \boldsymbol{X}_n \\ &= \Pi \circ \phi_{\Delta t} \boldsymbol{X}_n \\ &= \Pi \boldsymbol{X}_{n+1} \\ &= \boldsymbol{u}_{n+1} \end{aligned}$$

Spectral properties of DMD

$$\boldsymbol{u}_n = \sum_j a_i^1 \lambda_j^n \boldsymbol{\Phi}_i \equiv \sum_j \lambda_j^n \boldsymbol{\Phi}_i,$$

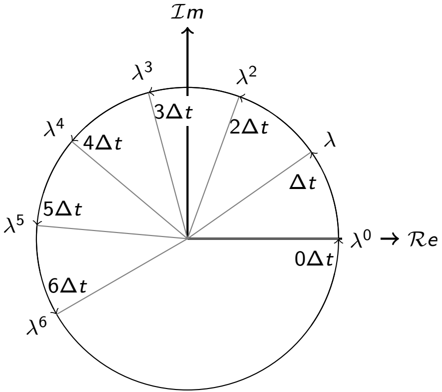

which means :

$$\lambda = \rho \exp\left(\sqrt{-1}\omega\Delta t\right).$$

Spatial properties inheritance [PoF2014a]

Let consider a spatial linear operator applied to the observable :

$$\nabla \cdot \boldsymbol{u}(\boldsymbol{r}, t) = 0$$

By injecting the modal decomposition :

$$\begin{aligned} \nabla \cdot \boldsymbol{u}(\boldsymbol{r}, t) &= \nabla \cdot \left(\sum_i \alpha_i(t) \boldsymbol{\Phi_i}(\boldsymbol{r})\right) \\ &= \sum_i \alpha_i(t) \nabla \cdot \boldsymbol{\Phi_i}(\boldsymbol{r}) \\ &= 0. \end{aligned}$$

Then, remembering $\alpha_j(t)$ form an orthonormal basis, we have :

$$\begin{aligned} \int_{-\infty}^{\infty} \alpha_j(t) \sum_i \times \alpha_i(t) \nabla \cdot \Phi_i(\boldsymbol{r}) \, \mathrm{d}t &= \int_{-\infty}^{\infty} \sum_i \alpha_j(t) \times \alpha_i(t) \nabla \cdot \Phi_i(\boldsymbol{r}) \, \mathrm{d}t \\ &= \sum_i \nabla \cdot \boldsymbol{\Phi_i}(\boldsymbol{r}) \int_{-\infty}^{\infty} \alpha_j(t) \times \alpha_i(t) \, \mathrm{d}t \\ &= \nabla \cdot \boldsymbol{\Phi_j}(\boldsymbol{r}) \\ &= 0. \end{aligned}$$

Henceforward, as for the observable $\boldsymbol{u}$, the divergence of each mode is zero.

– Comparison of 2D and 3D dynamic modes of the cavity flow –

Shear layer DMD mode [BIFD2013a,PoF2014a]

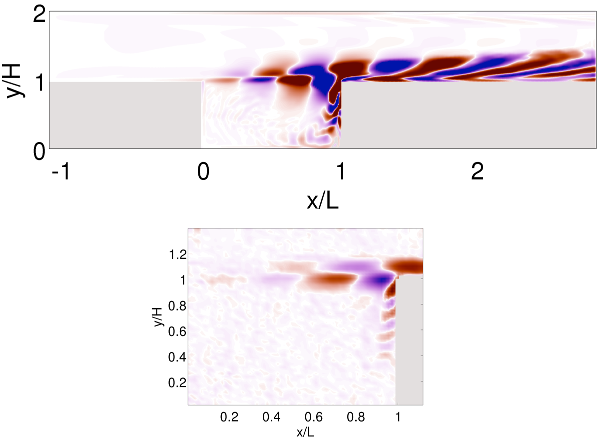

Shear layer DMD mode[BIFD2013a,PoF2014a]

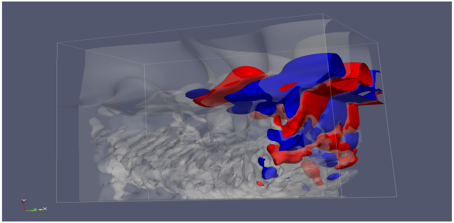

– Non-Uniform DMD (NUDMD) –

– Sampling constraint –

DMD and uniform sampling

The DMD algorithm needs an uniform sampling.

$$AK_1^N \equiv \{A\boldsymbol{u}_1, A\boldsymbol{u}_2, \ldots, A\boldsymbol{u}_N\} = \{\boldsymbol{u}_2, \boldsymbol{u}_3, \ldots, \boldsymbol{u}_{N+1}\} \equiv K_2^{N+1}$$

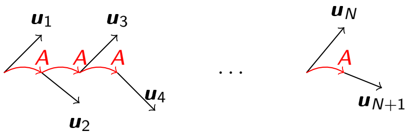

DMD and uniform sampling

Data problems

- Corrupted dataset
- Incomplete dataset
- Convergence of data pre/post-treatment

uniform sampling is not always possible

Experimental problems : example taken in Fluid Mechanics

Observable :
2D2C field (PIV) $\rightarrow 1000 \times 1000 px$
Frequencies of the flow :

1. one low ($\approx 0.1 Hz$) $\Rightarrow$ $10s$ of sampling at least
2. one high ($\approx 200 Hz$)$\Rightarrow$ sampling rate at $400 Hz$

Depth of images : 12-bit
Broad-band needed :
$bb = 400 \times 1000^2 \times 12 > 4 Gb.s^{-1}$
for at least $10s$

Unreachable for standard material

– Non-Uniform DMD –

Non-Uniform DMD [ICTAM2012,PoF2014b]

With the expression

$$\boldsymbol{u}_n = \sum_j a_i^1 \lambda_j^n \boldsymbol{\Phi}_i \equiv \sum_j \lambda_j^n \boldsymbol{\Phi}_i,$$

we can write more generally :

$$\begin{array}{lllll} \boldsymbol{u}_{t_n} & = & \sum_j \lambda_j^{t_n} \boldsymbol{\Phi}_j + \boldsymbol{e} & \approx & \lambda_1^{t_n} \boldsymbol{\Phi}_1 + \lambda_2^{t_n} \boldsymbol{\Phi}_2 + \dots \\ K & = & M\,V + R & \approx & M\,V. \end{array}$$

How to achieve this decomposition ?

$$K = M\,V + R \approx M\,V.$$

Pseudo-Vandermonde Matrix and Modes

V [3] is :

$$V = \begin{pmatrix} \lambda_1^{t_1} & \lambda_1^{t_2} & \dots & \lambda_1^{t_N} \\ \lambda_2^{t_1} & \lambda_2^{t_2} & \dots & \lambda_2^{t_N} \\ \vdots & \vdots & \ddots & \vdots \\ \lambda_{N_{\mathrm{md}}}^{t_1} & \lambda_{N_{\mathrm{md}}}^{t_2} & \dots & \lambda_{N_{\mathrm{md}}}^{t_N} \end{pmatrix},$$

and M is the modes :

$$M = \begin{pmatrix} \psi_1 \dots \psi_{N_{\mathrm{md}}} \end{pmatrix}.$$

3. times t_i are taken arbitrary, not necessary ordered.

How to achieve this decomposition ?

Obtaining of the Spatial Modes

Matrix M is easily computed :

$$M \approx K\, V^{+},$$

where V^{+} is Moore-Penrose pseudo-inverse of V.

Obtaining the frequencies 1/2 [ICTAM2012]

A frontal approach

M can be switched in equation $K = M\,V + R$. Then :
$K \approx K\,V^+\,V + R$. V can be computed by minimizing the residue matrix R[4] :

$$R \approx K\,\left(\mathcal{I} - V^+\,V\right).$$

The modes follows immediately through $M \approx K\,V^+$.

Drawback : computational cost, numerical instabilities.

4. K. Chen *et al.*, J. Nonlinear Sci. 22.6 (2012).

Obtaining the frequencies [PoF2014b]

Compressed computing

A low number of modes is supposedly dominant $\rightsquigarrow$ Temporal spectrum of the system is sparse.

- Compressed sensing approach [5] .
  - $\rightsquigarrow$ N_{md} modes are chosen.
  - $\rightsquigarrow$ only $\widetilde{N} \geq 2N_{\text{md}}$ are necessary.
- Clustering [6] components with similar spectral features, based on the sparse spectrum.
  - $\rightsquigarrow$ Select $\tilde{n}_p \ll n_p$ ones.

$\rightsquigarrow$ K is replaced by $\widetilde{K} \in \mathbb{R}^{\tilde{n}_p \times \widetilde{N}}$

5. D.L. Donoho *et al.*, (2006) *IEEE T. Inform. Theory*
6. n_p is the size of the observable, and K is $n_p \times N$

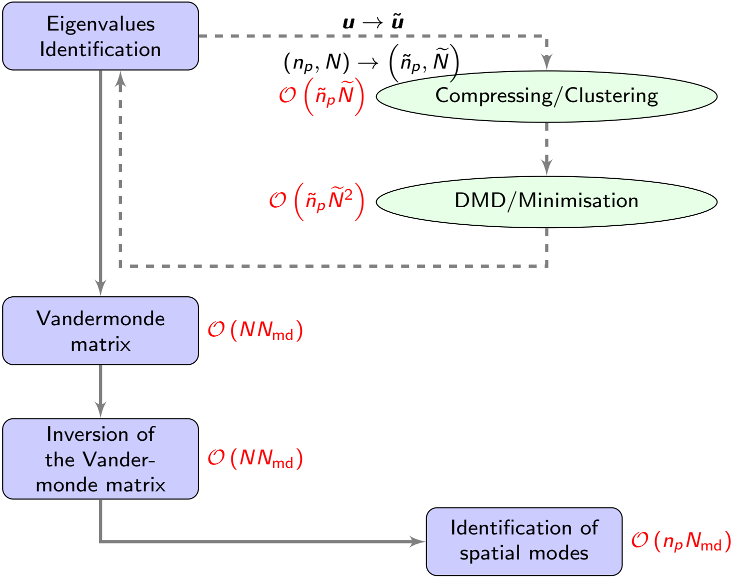
Eigenvalues Identification
$\boldsymbol{u} \to \tilde{\boldsymbol{u}}$
$(n_p, N) \to \left(\tilde{n}_p, \widetilde{N}\right)$
$\mathcal{O}\left(\tilde{n}_p \widetilde{N}\right)$
Compressing/Clustering
$\mathcal{O}\left(\tilde{n}_p \widetilde{N}^2\right)$
DMD/Minimisation
Vandermonde matrix
$\mathcal{O}\left(N N_{\mathrm{md}}\right)$
Inversion of the Vandermonde matrix
$\mathcal{O}\left(N N_{\mathrm{md}}\right)$
Identification of spatial modes
$\mathcal{O}\left(n_p N_{\mathrm{md}}\right)$

Synthetic case : frequency identification 2/2 [PoF2014b]

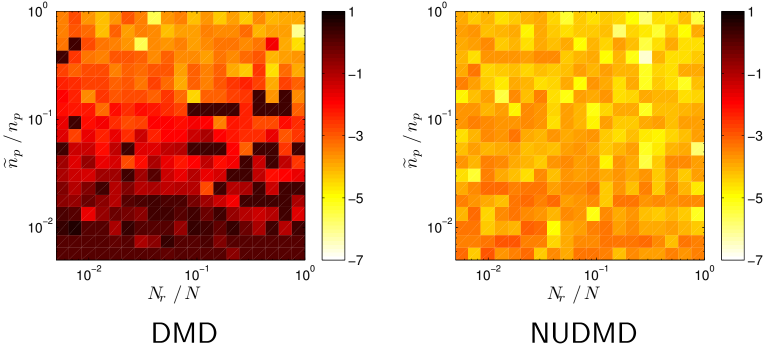

$$\epsilon_f = \left|\widehat{f} - f\right| / f$$

Synthetic case : growth rate identification [PoF2014b]

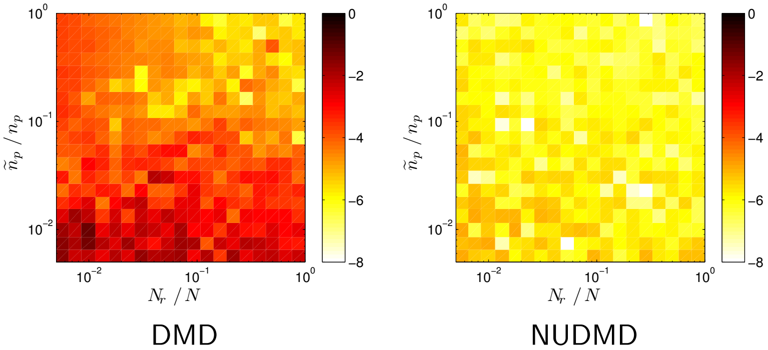

$$\epsilon_\sigma = \left| \widehat{\sigma} - \sigma \right| / \sigma$$

Illustration [ICTAM2012,PoF2014b]

Efficiency of compressed approach

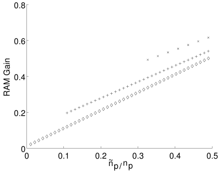

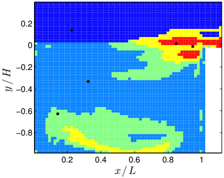

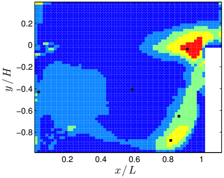

Illustration [ICTAM2012,PoF2014b]

Results on the cavity flow

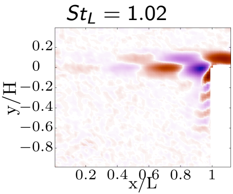

DMD mode
500 snapshots
7000 spatial points

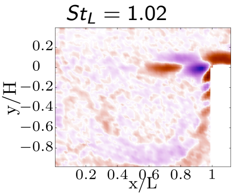

NU-DMD mode
10 randomly taken snapshots
7000 spatial points

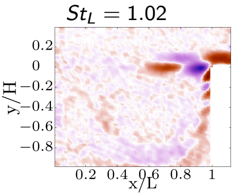

NU-DMD mode
10 randomly taken snapshots
10 spatial points

– DMD-Observability –

If we consider time series $\tilde{\boldsymbol{u}}$ extracted from $\boldsymbol{u}$ [7], we can write the automatic system :

$$\begin{cases} \boldsymbol{u}_{n+1} & = & A\boldsymbol{u}_n \\ \tilde{\boldsymbol{u}}_n & = & C\boldsymbol{u}_n \end{cases},$$

Then the system is observable ($\boldsymbol{u}_0$ can be reconstructed from the n_p first $\tilde{\boldsymbol{u}}$) if the Kalman matrix has a full rank :

$$\mathcal{K} = \begin{pmatrix} C \\ CA \\ \vdots \\ CA^{n_p-1} \end{pmatrix}.$$

Practically, the conditioning of A^i is blowing up, so it is undoable to estimate the observability qualities of time series with the Kalman Matrix.

7. where $\boldsymbol{u} \in \mathcal{R}^{n_p}$

" When you think about a variable, the evolution of it must be influenced by whatever others variables it's interacting with. Their values must somehow be contained in the history of that thing. Somehow their mark must be there. "

James Farmer, (1986) *Interview with James Gleick*

J.D. Farmer *et al.*, "Geometry from a time series", (1980), *PRL*

" When you think about a variable, the evolution of it must be influenced by whatever others variables it's interacting with. Their values must somehow be contained in the history of that thing. Somehow their mark must be there. "

James Farmer, (1986) *Interview with James Gleick*

J.D. Farmer *et al.*, "Geometry from a time series", (1980), *PRL*

Propagation of the field

$\boldsymbol{u}_{n+1} = A\boldsymbol{u}_n$:

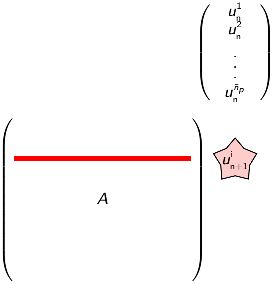

The number of elements on the ith line allows to count points influential in the dynamics of the observable $\{u^i\}$

DMD-observability criterion [RNL2013]

Then, by counting the number of significant components of A :

- n_l on the ith line
- n_c on the *ith* column

we define the DMD-observability for the ith component as :

$$\sigma_\alpha(i) = \frac{1}{n_p}\left(\alpha n_l + (1-\alpha)(n_p - n_c)\right)$$

We can approximate the operator A, thanks to the DMD algorithm :

$$A \approx K_1^N S K_1^{N^{-1}}.$$

– Illustration –

Illustration on a cavity flow [RNL2013]

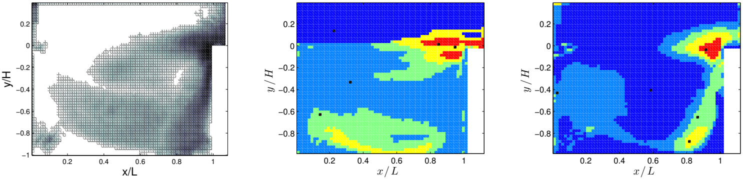

Good agreement with experimental placement of sensors and with Basley [8] .

8. J. Basley, 2012, *PhD thesis*,2014,*J.Fluid Mech.*

– Identification of Lagrangian Structures –

Material frontier

Dynamical flow : $\vec{\boldsymbol{X}}(t) = \phi^t\left(\vec{\boldsymbol{X}}(0)\right)$
Invariant manifolds are invariant through the flow.
Consequently : such a manifold is a material frontier.

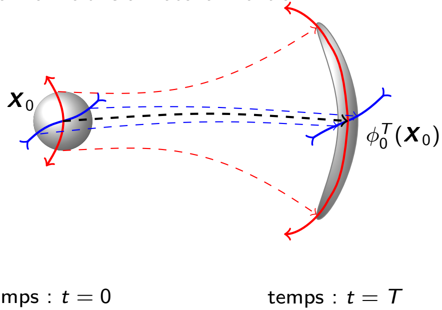

Stretching of fluid particles

How to identify these manifolds ?

Fluid particles are deformed by manifolds.

Miller *et al.*[9] and Haller *et al.*[10] had proposed to look at the stretching of fluid particles.

$$\delta X\left(T\right)=\frac{\mathrm{d}\phi^{T}\left(X\right)}{\mathrm{d}X}\delta X\left(t_0\right)=J\delta X\left(t_0\right)$$

9. Miller *et al.*, (1997) *Physica D*
10. Haller *et al.*, (1998) *Physica D*, (2000) *Chaos*, (2005) *J. Fluid Mech.*

Cauchy Green Tensor

Quantifying the stretching is done by the evaluation of the Cauchy Green Tensor [11] :

$$\boldsymbol{C} = J \times J^{\dagger}$$

Then, the particule deformation rate is driven by the maximum eigenvalue of $\boldsymbol{C}$, *i.e.* Finite-Time Lyapunov Exponent of the flow [12] .

11. Haller *et al.*, (1998) *Physica D*, (2000) *Chaos*, (2005) *J. Fluid Mech.*
12. S.C. Shadden,*et al.*, (2005) *Physica D*

Lagrangian Coherent Structures

In autonomous/periodic system : invariant manifolds create ridges in the FTLE field.

In non autonomous system, there is non uniqueness of manifolds. Nevertheless, the ridges are still (most of the time) material frontier, and drive the mixing.

Ridges are called *Lagrangian Coherent Structures*.

Illustration

Attractive (red), repulsive (blue) LCS and vorticity field.

Illustration [BIFD2011,2013b]

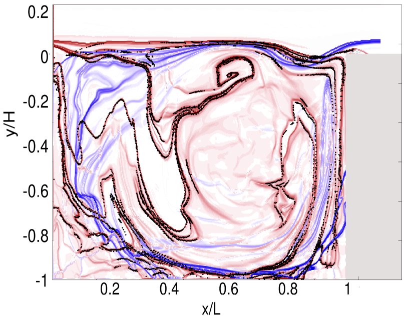

Black dots are virtual particles.

Illustration [BIFD2011,2013b]

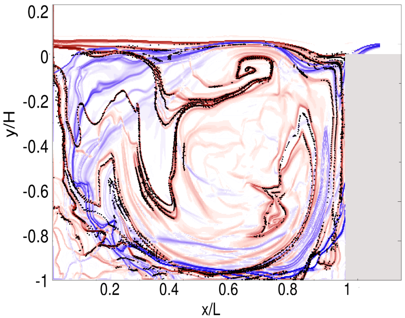

Black dots are virtual particles.

Illustration [BIFD2011,2013b]

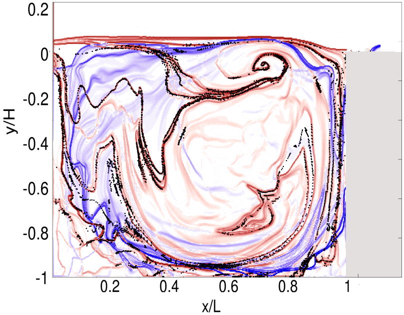

Black dots are virtual particles.

Illustration [BIFD2011,2013b]

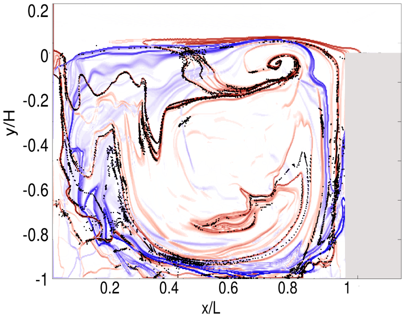

Black dots are virtual particles.

Illustration [BIFD2011,2013b]

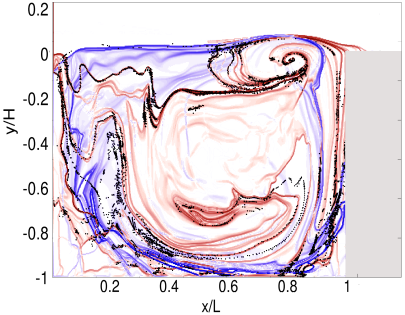

Black dots are virtual particles.

Forward and backward LCS

Qualitative results

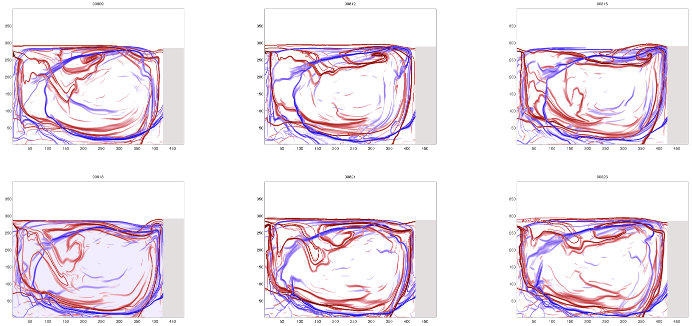

Simplification of the flow

DMD and Restricted Reduced Order Model

We build a synthetic flow, based on a Dynamical Modes Decomposition analysis of the dataset :

$$\boldsymbol{u}_{\boldsymbol{ROM}}\left(\boldsymbol{r},t\right)=\bar{\boldsymbol{u}}\left(\boldsymbol{r}\right)+\mathcal{R}e\left(\mathrm{e}^{i\omega t}\boldsymbol{\Phi}_{\omega}\left(\boldsymbol{r}\right)\right)$$

where $\boldsymbol{\Phi}_{\omega}$ is the dominant shear layer DMD mode.
The periodicity of the model is important : Now one can see LCS structures as invariant manifolds in a Poincarré' section.

Verification of relevance

Comparison with real flows

ROM flow structures (top) and real flow structures (bottom), with similar horizon.

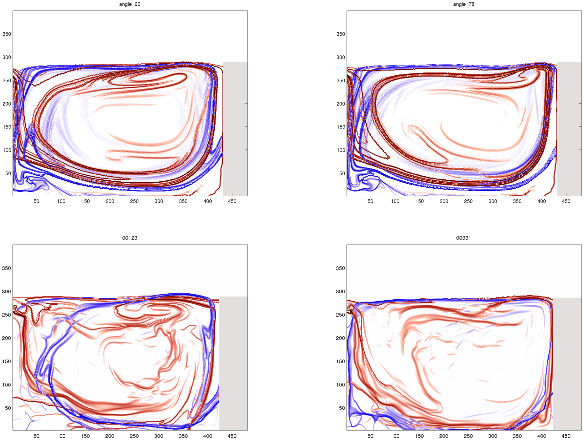

Simplification of the flow (2/3)

Invariant manifolds of the model

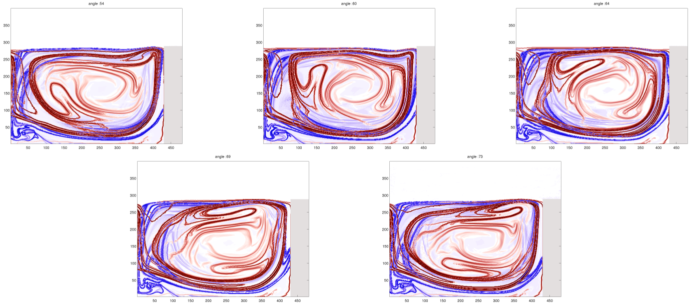

Simplification of the flow (3/3)

Horse-Shoes

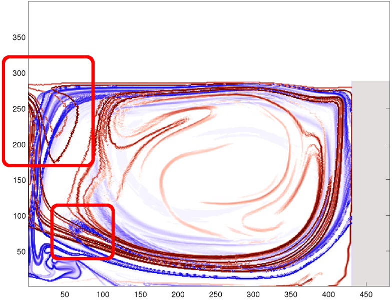

– Conclusions –

Conclusions

- Methods for extracting spectral informations of the dynamics, fitted for ill-conditionned dataset[1–4].
- Identification of representative points[1]
- Equation-free criterion for estimation the observability qualities of observable[5].
- FTLE field computations[6–8].
- Exploration of a cavity flow properties[1,2,4–8].

Some publications

1. *A Dynamic Mode Decomposition approach for large and arbitrarily sampled systems*, in revision for PoF, 2014
2. *Investigating mode competition and 3D features from 2D velocity fields in an open cavity flow by modal decompositions*, PoF 26, 2014
3. *POD-Spectral Decomposition for Fluid Flow Analysis and Model Reduction*, TCFD 27, 2013
4. *Snapshot-Based Flow Analysis with Arbitrary Sampling*, ICTAM 2012
5. *DMD économique pour l'identification de structures dans des écoulements 3D*, RNL 2013
6. *Fast Identification of Lagrangian Coherent Structures*, BIFD 2011
7. *GPU and SIMD Acceleration for Identification of Lagrangian Coherent Structures. Application to an Open Cavity Flow*, BIFD 2013
8. *Lagrangian Coherent Structures in Open Cavity Flows*, ETC 2013

More infos available on my website :

`www.gueniat.fr/publications.html`

Future Works

- Minimization-free methods.
- Building a theoretical link between DMD decomposition (*i.e.* "Koopman operator") and Lagrangian structures (*i.e.* "Perron-Frobenius operator").
- Derive a theoretical framework around the DMD observability, and improve the criterion.

I am currently working on :

- Construction of sparse and pertinent representations of dataset/dynamics.
- Efficient computations of these representations.
- Control of the systems, thanks to these representations.
- (Computer Human Interfaces, in augmented/virtual reality, for 3D data exploration.)

Sparse representations of a dataset and efficient computations

A hash function $\mathfrak{h} : \mathcal{R}^{n_e} \rightarrow \mathcal{N}$ associates an entry $\boldsymbol{u}$ with a *key* k.
Keys are associated to clusters in the phase space.

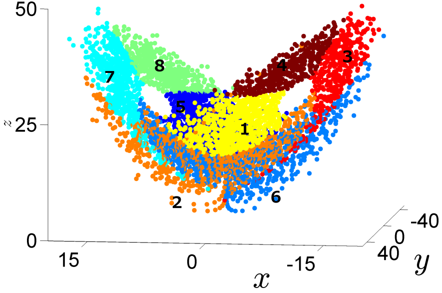

- ✓ every kind of observable (even 1-D)
- ✓ Very computational friendly

Control of the dynamics

Using dynamic programming, it is possible to learn how to control semi-automatically the transition probabilities from one cluster to another :

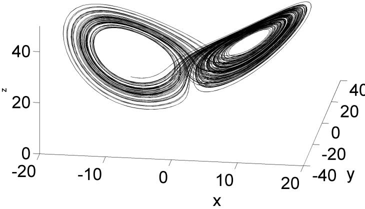

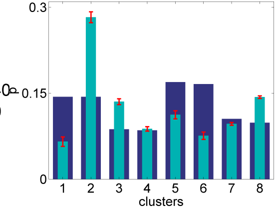

Thank you for your attentiveness.
If you have any questions, I will be pleased to answer those.